Journal of Energetic Materials
Publication details, including instructions for authors and subscription information:
http://www.informaworld.com/smpp/title~content=t713770432

Wettability of Ammonium Nitrate Prills

Queenie S. M. Kwok[a]; Peeter Kruus[b]; David E. G. Jones[a]
[a] Canadian Explosives Research Laboratory, Natural Resources Canada, Ottawa, Ontario, Canada [b] Department of Chemistry, Ottawa, Ontario, Canada

Online publication date: 17 August 2010

To cite this Article Kwok, Queenie S. M. , Kruus, Peeter and Jones, David E. G.(2004) 'Wettability of Ammonium Nitrate Prills', Journal of Energetic Materials, 22: 3, 127 — 150
To link to this Article: DOI: 10.1080/07370650490522776
URL: http://dx.doi.org/10.1080/07370650490522776

Energetic Materials, 22: 127–150, 2004

ISSN: 0737-0652 print
DOI: 10.1080/07370650490522776

Taylor & Francis
Taylor & Francis Group

Wettability of Ammonium Nitrate Prills

QUEENIE S. M. KWOK

Canadian Explosives Research Laboratory,
Natural Resources Canada
Ottawa, Ontario, Canada

PEETER KRUUS

Department of Chemistry, Carleton University,
Ottawa, Ontario, Canada

DAVID E. G. JONES

Canadian Explosives Research Laboratory,
Natural Resources Canada
Ottawa, Ontario, Canada

The wettability of ammonium nitrate (AN) prills is one of the primary factors determining the physical stability and detonation behavior of ANFO. The wettabilities of various types of AN prills were compared using capillary penetration measurements. Complementary characterization studies using scanning electron microscopy (SEM) and thermogravimetry (TG) were performed to rationalize the observed differences in wettability. The wettability of AN was found to be affected by several factors, including surface tension, viscosity, density, and purity of the liquid used, as well as surface composition, porosity, bulk density, particle size, moisture content, and thermal history of the AN samples.

Keywords: ammonium nitrate, ANFO

Address correspondence to Queenie S. M. Kwok, Canadian Explosives Research Laboratory, 555 Booth Street, Ottawa, Ontario, Canada K1A 0G1. E-mail: qkwok@nrcan.gc.ca

Introduction

ANFO, an admixture of ammonium nitrate (AN) prills with fuel oil, is widely used as a commercial explosive. A mixture of 94 mass % AN prill and 6% liquid hydrocarbons (mostly No. 2 diesel fuel) makes a practical and cost-effective blasting agent. This optimum ratio provides the maximal theoretical energy, highest detonation velocity [1], highest sensitivity, high efficiency, and minimal postblast toxic fumes [2]. The ability of AN to adsorb liquid fuel is one of the primary factors determining the physical stability, detonability, and detonation parameters of ANFO [1, 3]. However, limited published information is available on the surface and interfacial properties of AN and fuel oil. This research explores the effects of several factors on the wettability of the inorganic salt AN with a variety of organic liquids.

Pure AN crystals have several phase transitions [4], as illustrated in Figure 1. Beside the phase transitions between the adjacent solid phases, a metastable phase transition II–IV can also occur at 50°C (Figure 1). After cycling through these temperatures, AN prills may have a different volume and structure. The two temperatures at which cycling will occur under normal Canadian conditions are 32 and −18°C when the prills are stored in rail cars or silos. Practical problems are observed when AN prills are cycled through these two phase transitions during transportation and storage. This research also explores the effects of these phase transitions on the wettability of AN prills.

The success of the wetting process is determined by the physicochemical surface properties of the interacting surface components, and particularly the wettability of the components. There are several strategies for quantitative assessment of the wettability of solid materials [5, 6]. Direct contact angle measurement is a simple and economical approach to study the wettability of

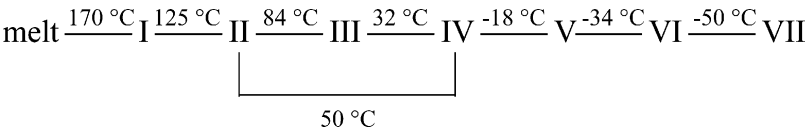

Figure 1. Phase transitions of AN.

materials [5]. However, these direct techniques are not applicable to powders and porous materials. Thus, the capillary penetration technique, an indirect approach to contact angle measurements, has been developed and applied to determine the wetting characteristics of a variety of powders or porous materials [7, 8].

The capillary penetration technique is based on the rate of liquid penetration into packed beds of particles. The basic equation that describes the kinetics of penetration of liquids into powder or porous bodies was developed by Washburn [9] and modified by Siebold et al. [10]:

$$M^2 = \frac{K\rho^2\gamma_{\mathrm{lv}}\cos\theta}{2\eta}\,t, \tag{1}$$

where M is the mass of the liquid that penetrates into the capillary system at time t, θ is the contact angle between the liquid and particle, and ρ, γ_{lv}, and η are the density, surface tension, and viscosity of the liquid, respectively. K is the geometric factor of the packed beds of particles, which depends on the cross-sectional area, radius, and porosity of the column of packed particles. Equation (1) neglects the effects of slip, gravity, and inertial effects and assumes there are no external pressure gradients.

This research explores the possible application of capillary penetration measurements to determine the wettability of AN prills with various hydrocarbons and fuel oil, and subsequently the wettability of the AN prills from different sources. Complementary characterization studies using scanning electron microscopy (SEM) and thermogravimetry (TG) were performed in an attempt to rationalize the observed differences in particle wettability.

Experimental

Ammonium Nitrate

Five samples of AN prills from three different categories were used in this study, identified as Types A–E. Their categories, bulk density, void fraction, prill size range, and prill size distribution are summarized in Table 1. The bulk density, which was calculated using the sample mass and volume in a cylinder,

Table 1
Characteristics of various AN prills and their wetting rate with heptane

Type	Category	Bulk density/ $g\,cm^{-3}$	Void fraction	Prill size/ mm	Mass % with prill diameter/mm[a]					External surface	Internal surface	10^3 Wetting rate/ $g^2\ min^{-1}$
					>2.0	1.7–2.0	1.4–1.7	1.0–1.4	<1.0			
A	Porous	0.83 ±0.01	0.48 ±0.01	0.9–3.0	34	41	10	14	1	O, N, S, Al, Si, P	O	2.68 ± 0.05
B	Porous	0.75 ±0.01	0.55 ±0.01	1.2–3.0	52	46	1	1	0	O, N, Ca, S, P, Al	O	2.26 ± 0.22
C	Porous	0.76 ±0.01	0.52 ±0.01	1.2–3.0	95	5	0	0	0	O, N, S, Ca, Al	O	2.39 ± 0.18
D	Mini	0.97 ±0.01	0.43 ±0.01	0.7–1.3	0	0	0	0	100	O, N, P	O	1.20 ± 0.15
E	Dense	0.91 ±0.01	0.43 ±0.01	1.8–3.4	98	2	0	0	0	O, N, P	O, N, P	0.67 ± 0.02

[a]Values correspond to mass % of prills within the specific sizes range, expressed in mm.

refers to the density of the prills, including pores and interprill spaces. The void fraction was determined by the volume of octane added to a cylinder packed with AN prills. The size distribution of the samples was determined by sorting the prills through sieves of various sizes. All the prills used in this study are commercial AN prills with additives and/or coating agents (e.g., kaolinite, talc). The type and the amount of additives and/or coating agents, as well as the previous thermal history of each individual sample, are unknown. Unless specified otherwise, the samples were used as received. All the prills were stored under identical conditions before measurements.

Liquids

A series of pure organic liquids (heptane, octane, nonane, dodecane, and hexadecane) was used as wetting liquids, as listed in Table 2. Except for fuel oil (diesel fuel), all other liquids were reagent-grade straight-chain isomers with a purity of at least 98%. The suppliers are listed in Table 2. The fuel oil was obtained from a local gas station. All chemicals were used without further purification.

For the various wetting liquids, their surface tension (γ_{lv}), density (ρ) and viscosity (η) measured at 23°C are listed in Table 2. The surface tension was measured using a CENCO-DuNOUY Interfacial Tensiometer (Central Scientific) and the viscosity with a Cannon-Fenske Routine Viscometer (Industrial Research Glassware Ltd.). The density was determined by weighing 10 mL of the corresponding liquids.

Sample Preparation

Two types of AN powders were obtained by (1) grinding Type A AN prills using an IKA model A10 analytical mill, and (2) breaking down temperature-cycled (T-cycled) prills.

T-cycled prills were prepared by heat- and cold-treating Type A AN prills. The samples were first put into an oven (Fisher Scientific Co.) at 60°C for 12 hr, then restored to room temperature for an hour, and finally placed in dry ice (∼−78°C) for 5 hr. This cycle was repeated twice.

Table 2
Capillary penetration results for type A AN prills with various liquids

Liquids	Supplier[a]	γ_{lv}/mJ m^{-2}	ρ/g cm^{-3}	η/mPa·s	10^3 Wetting rate/ g^2 min^{-1}
Heptane	F	21.4	0.678	0.405	2.83 ± 0.10
Octane	A	22.6	0.698	0.528	1.97 ± 0.18
Nonane	A	23.4	0.715	0.687	1.24 ± 0.04
Dodecane	A	26.4	0.747	1.403	0.70 ± 0.04
Hexadecane	A	27.8	0.770	3.159	0.42 ± 0.04
Fuel oil	G	30.5	0.820	1.765	1.16 ± 0.33

[a]A: Aldrich Chemical Inc.; F: Fisher Scientific Co.; G: local gas station.

Cold-treated prills were prepared by two different approaches: (1) placing the prills in dry ice for 5 hr, and (2) storing the prills in a domestic freezer ($\sim -22°C$) for 3 weeks.

Heat-treated AN prills were prepared by putting Type A prills in an oven (Fisher Scientific Co.) at 60°C for 12 hr.

Moisturized AN prills were prepared by placing Type A prills under a bell jar with a pot of water. Samples with different moisture content were obtained by exposing the samples to water vapor for 1.5–24 hr. The relative humidity (R.H.) of air in the system was 70–80% as measured by a humidity meter. The moisture content of each sample was verified using TG.

Capillary Penetration Measurements

The approach is based on measuring mass as a function of time of a liquid wicking up through a packed bed of particles contained in a tube. The experimental setup for a capillary penetration measurement is shown in Figure 2. About 5.0 g of AN samples were packed in a glass tube. The inner diameter and the length of the glass tube were 1.08 and 15 cm, respectively.

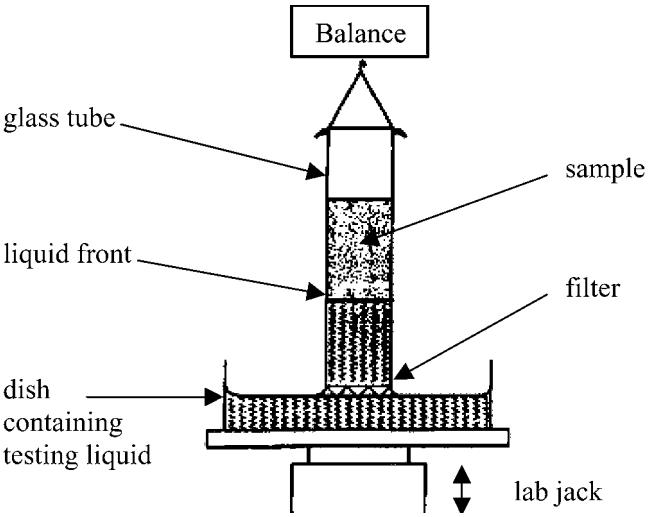

Figure 2. Setup for capillary penetration technique.

The lower end of the tube was closed by a stainless steel filter, which was cut from a coffee filter. The column packed with samples was then dipped in a glass dish (volume of 50 mL and diameter of 10 cm) filled with the appropriate testing liquid. The penetration rate of the liquid into the samples was determined by monitoring the column mass gain as a function of time. Depending on the nature of both sample and liquid, an experiment took from 30 to 140 min.

An essential requirement for reproducible measurements is the uniform and reproducible packing of the tube with AN particles. The packing procedure was run as follows: the tube filled with the 5.0 g of sample was first dropped 20 times from a height of about 20 cm, and then was vibrated for 5 min with an electric vibrator (constructed from a shaver). The time required to pack the tube was set at 5 min, since after 4 min, the height of the samples was constant. Prior to each run, the packing constant (bulk density) was calculated, to ensure a consistent packing for each type of sample.

Temperature as well as R.H. in air near the column were recorded to make sure that their variations were limited: $23 \pm 3°C$ and $39 \pm 18\%$ R.H. Although the variation of R.H. was large in the whole duration of the study, there was no significant difference in the results for the same sample at 21% and 60% of R.H.

Scanning Electron Microscopy

The external and internal structures of various AN prills were examined by SEM, model JSM 6400 (JEOL Ltd.). The external structure of the prills was examined on unbroken prills, and the internal structure was observed in cleaved prills. The cleaved prills were prepared by cutting prills into halves with a sharp blade. The samples were mounted on specimen studs using double-sided adhesive tape, and were coated with a gold-palladium alloy. The SEM observations were conducted at low accelerating voltage (3 or 8 kV) to minimize the beam damage to the samples.

An energy-dispersive (ED) X-ray spectrometer attached to the SEM was used to chemically analyze small selected areas

of various AN prills. Al Kα X-rays were used as an X-ray source in a vacuum of 1×10^{-9} Torr. For the X-ray microanalysis, the specimen studs mounted with samples were coated with carbon.

Thermogravimetry

The water content of the as-received and as-prepared AN prills was established by a TA Instruments 2950 TG accompanied with a TA 5200 Thermal Analysis System. The sample was heated from 25 to 110°C at 5°C min^{-1}. A platinum pan containing about 30 mg of AN prills was purged with dry nitrogen at a flow rate of 60 mL min^{-1} in the furnace and 40 mL min^{-1} in the balance chamber.

Results and Discussions

Wetting Rate of Various Liquids with AN

A typical result obtained from a capillary rise measurement for an AN-packed column is illustrated in Figure 3, where M^2 of the column is plotted versus t. According to the modified Washburn equation (equation 1), M is predicted to be a square root function of t. However, all the results obtained in this study show a parabolic increase of M^2 with time during the initial period. In some experiments downward deviations from the straight line were also observed at longer times near the end of the runs. The nonlinearities in the experimental M^2 versus t relationship may be due to the inappropriateness of the assumptions in the Washburn equation.

The effect of inertia is considered negligible, and laminar conditions are assumed to set up very rapidly in the Washburn equation. However, Quéré [11] has shown that at the early stage, the capillary penetration is governed by inertial forces, and the transition time from an inertial to viscous regime is given by $\tau = \rho R^2/4\eta$. In this study the initial unsteady state is observed for all the liquids tested, and the extent of this domain seems to depend on the liquid. However, the observed deviations do not agree with the above relationship of transition time. Apparently the deviations at the early stage of the experiments may also depend on other factors, for

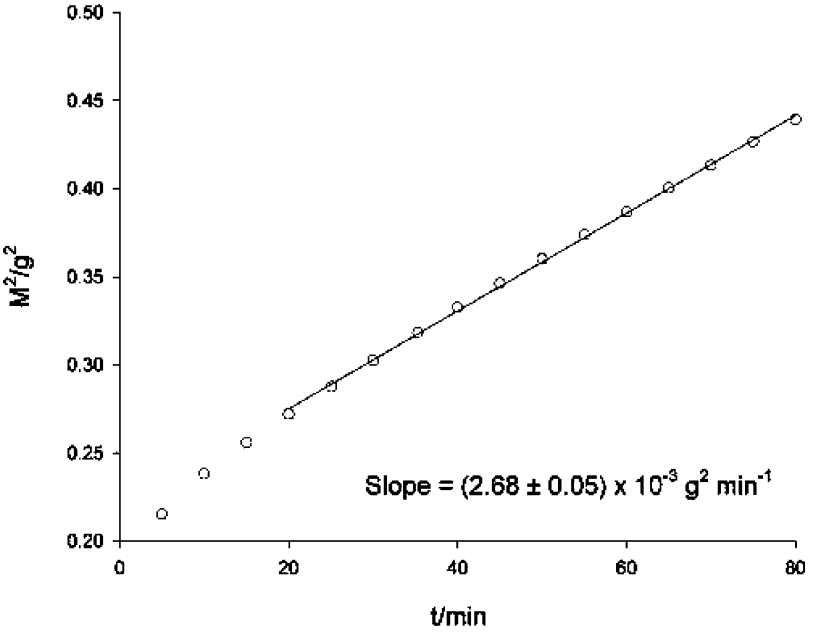

Figure 3. Capillary penetration results for AN prills with heptane.

example, mass gain data may be affected by the liquid wicking on the internal wall of the glass tube.

Furthermore, the Washburn equation does not include the effect of gravity, which tends to decrease the forwarding of the liquid. An increasing height of the liquid front increases the influence of gravity, leading to a deviation of the experimental behavior. According to Washburn [9], the gravity effect can be neglected until $h \approx 0.1 \ H_{eq}$. The maximum height ($H_{eq} = 2\gamma_{lv}\cos\theta / R\rho g$) of the liquid front reached in infinite time, when capillary and hydrodynamic forces are equal at equilibrium, is controlled by gravity (g).

In this work deviations were not observed in most of the experiments, in which the height of the penetrated liquid at the end of each run was usually less than 4 cm. Small deviations downwards from the straight line were observed near the end of

some experiments, which imply that gravity needs to be taken into account when the liquid height is greater than 4 cm.

Mass loss due to the evaporation of the adsorbed liquids on AN samples may also cause deviation from the Washburn equation. However, in this study the samples were contained in a glass tubes and the liquid vapor can escape from the system only through the open end of the tube (see Figure 2). Since the vapor of the most volatile liquids could be readsorbed by the prills on the top, the evaporation effect of the testing liquid should be negligible.

In each experiment the wetting rate (M^2/t) is estimated from the slope of a linear regression on the selected (M^2, t) data domain (Figure 3). This domain is selected from the region of the curve where its tangent has the least slope variation, that is, where the effects of inertia and gravity seem to be negligible.

Capillary penetration measurements on Type A AN prills were conducted with various testing liquids, including a series of alkanes and fuel oil. The average values of the wetting rates determined from two to three replicates are summarized in Table 2. The error term of the values represents one standard deviation determined from the repeated experiments.

As compared in Table 2, the wetting rates of the alkanes decrease with increasing γ_{lv}, ρ, and η of the liquids, in agreement with the Washburn equation. However, the results also suggest that fuel oil has a higher wetting rate on AN, while its γ_{lv}, ρ, and η are also higher than dodecane. Since fuel oil is a mixture of alkanes and aromatic hydrocarbons, the higher wettability of fuel oil with AN may be due to the higher attractive interaction of some of its components with the AN surface. On the other hand, a poorer reproducibility of wetting rates was also obtained from fuel oil (error $\pm 28\%$) than from alkanes (error $\pm 10\%$). The variations in the wetting rate data may be due to nonuniform and preferential penetration of fuel oil. Each of the components has a different penetration rate, and the composition of the fuel oil may vary as it rises. The poor reproducibility and variation in wetting rate indicate the potential problems during wettability testing with mixtures. It is thus important to use pure probe liquids in the capillary penetration measurements.

The main deficiency of the model derived from the Washburn equation is that only a single cylindrical capillary is used to characterize a complex porous network. Hence, the method cannot be used to predict the exact process of the liquid penetration in AN prills. However, given the simplicity of the capillary penetration technique, it can be used as a valuable alternative to estimate the wetting rate. The obtained wetting rates serve as an empirical measure to compare the relative wettability of various AN prills.

Wettability of Various AN Prills

The wetting rates with heptane of the as-received AN prills were measured using the capillary penetration technique. As seen in Table 1, there are significant variations in the wettability of the various AN samples. Among the five samples, Type A AN prills have the highest wetting rate with heptane. For Types B and C prills, the wetting rates are similar and lower than that for Type A prills by about 13%. The wetting rates for Types D and E prills are much lower than those for porous prills (Types A–C); they are, respectively, 55% and 75% lower than that observed for Type A prills.

The wetting process for AN is a function of the solid and liquid characteristics, as well as the solid-liquid interactions. Since the wetting rates of the five samples were measured using the same wetting liquid, the variations in their wettability are mainly due to the differences in their characteristics.

Effect of Morphology and Porosity. SEM was used to determine the external and internal surface morphology for the various AN prills. As presented in Figure 4, the external surfaces of Types A, B, and C AN prills are not smooth, and they have a nonuniform distribution of pores over their external surface. Comparing the three porous prills (Figure 4a–c), there are slight differences in their surface openings. Type A prill has a channeled pore structure (Figure 4a). Types B and C have characteristic growth on the external surface that covers the pore structure (Figure 4b and c).

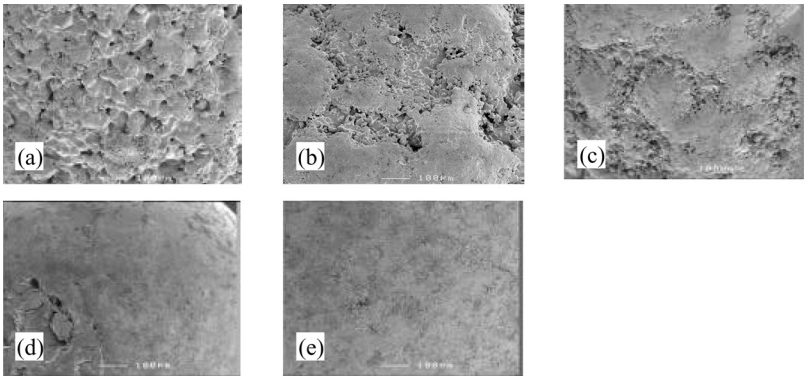

Figure 4. SEM micrographs on external surface of AN prills (all ×150): (a) A, (b) B, (c) C, (d) D, (e) E.

As depicted in Figure 5a, all the AN porous prills (Types A–C) have an internal central hollow. Their internal structure, as shown in high-magnification micrographs in Figure 6, indicate that there are differences in the particle shape. Type A prill has a pore structure in which the grains are connected (Figure 6a). Type B prill has an internal structure composed of nodular-shaped (spheroid) particles with an irregular distribution of pores (Figure 6b), whereas Type C prill consists of oriented dendritic particles with channel pores (Figure 6c). The SEM micrographs suggest that the external and internal pore sizes of porous prills range from 10 to 80 μm.

Typical SEM micrographs of Types D and E AN prills are also presented in Figures 4–6. The external morphology of

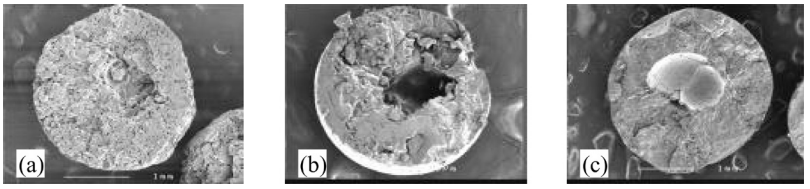

Figure 5. SEM micrographs on internal surface of AN prills: (a) A–C (×35), (b) D (×70), (c) E (×30).

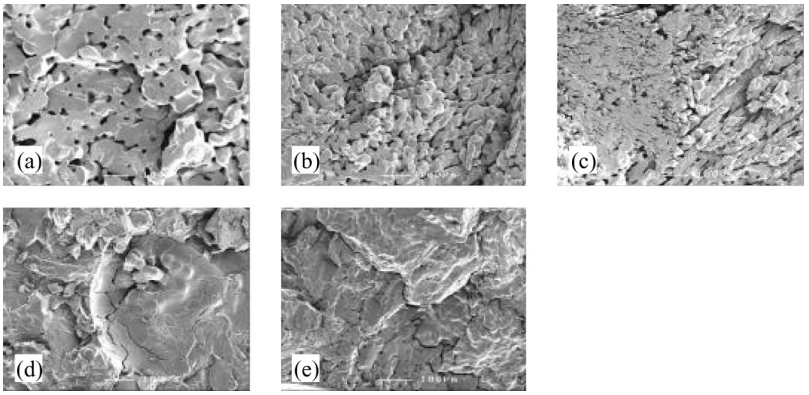

Figure 6. SEM micrographs on internal surface of AN prills (all×150): (a) A, (b) B, (c) C, (d) D, (e) E.

Types D and E prills is shown as a highly dense structure with very few surface pores in Figures 4d and 4e. For Types D and E prills, although the central hollow is distinctly formed (Figures 5b and 5c), there are no channels linking it to the external surface. From the general internal micrographs of Types D and E prills (Figure 6d and 6e), it can be observed that the prills have a continuous solid mass, which is interrupted by a few discrete pores. The approximate maximum pore sizes for Types D and E prills are 8 and 10 μm, respectively.

Both the external and internal surfaces of Types D and E prills are much finer than the porous prills (Types A–C). The pore sizes for Types A, B, and C prills are 10 times larger than those for Types D and E prills. The relatively high porosity of Types A, B, and C prills contribute to their enhanced wettability (see Table 1). Among the porous prills, Type A prills have the highest wettability, which may be the result of a higher porosity. However, SEM is only able to sample surface pores within a small viewing area, and it is insufficient for evaluating the percentage of pore structure.

At present, there are various methods for characterizing porous materials; however, among these methods, only electron microscopy and mercury porosimetry are suitable to describe

the pore size range of AN prills (>1 μm). Mercury porosimetry has been shown to assess incorrectly the overall pore geometry and the distribution of pores in AN prills [12]. Nuclear magnetic resonance microscopy [12] and high-resolution thermogravimetry [13] have been applied to characterize the structural properties of porous AN prills. Further comparison of the three porous prills (Types A–C) may be carried out using these techniques.

Effect of Surface Composition. X-ray microanalysis was used to characterize the surface chemistry of the individual samples of AN prills. Spectra of the AN samples contain signals due to the elements of carbon, nitrogen, oxygen, phosphorous, sulfur, aluminum, silicon, and calcium. The signal of carbon was mainly from the carbon coating of the samples prior to the measurements. No quantitative analysis was performed; however, the relative quantity of each element was determined by comparing the intensities of the lines. The results for the sample are summarized in Table 1; the elements are listed in order from highest to the lowest intensities. Evidently, besides the major constituents of AN (oxygen and nitrogen), some other elements are also present on the surface of the prills. It is not surprising to find these elements, because different coatings and additives (e.g., kaolinite, talc) are added to prevent the adsorption of moisture by AN.

The X-ray microanalysis results in Table 1 suggest that qualitatively Types D and E prills have less impurity on the surface. However, a strong signal of phosphorous was obtained from Type E prills. Additionally, since the surface chemistry was analyzed by a small spot X-ray microanalysis on a selected area of AN samples, the results may not be representative of the complete sample.

The internal surfaces of the cleaved AN prills were analyzed using X-ray microanalysis, with the option of ''area scan.'' The area analyzed was about 0.16 mm^2, which was approximately 100 times larger than that for the external surface analysis, but the depth of samples analyzed was lower. The results in Table 1 suggest that there may be less impurity on the internal surface of the prills. Moreover, there was no nitrogen detected from

the internal surface of Types A–D prills. Apparently oxygen occupies the most outer layer of cleaved surface of the prills. Since AN is very hygroscopic without the additives, the surface of the cleaved prills may have a higher tendency to adsorb water. Hence, the signal of oxygen may also result from adsorbed water, which was confined between the surface of the cleaved prills and the carbon coating.

Surface impurities affect surface wettability of AN prills. To determine the effect of coatings or additives on the wetting of AN prills, comparison of AN prills with and without coating is required. However, AN is very hygroscopic without the coating. Hence, it would be difficult to eliminate the effect of moisture and to obtain valid results from capillary penetration measurements. Alternatively, wettability studies on the coating and additives used per se may provide hints as to their effects on the wettability of AN.

Effect of Bulk Density. The bulk density, void fraction, and prill size distribution for various AN prills are summarized in Table 1. The bulk density of AN prills depends upon the shape of the prills, their density, the geometrical arrangement, as well as the void fraction. Theoretically, for uniform-sized spheres, the void fraction varies from about 0.26 to 0.48 for different types of packing, from 100% rhombohedral to 100% cubic. The void fractions of Types A, D, and E prills fall within these two values, but toward the higher value because of nonuniform sized spheres and random arrangement of the samples. Types B and C prills have a higher void fraction, which may result from the nonuniform spherical shape of the porous prills.

Among the porous prills, sample A has the lowest void fraction and highest bulk density, due to the wider distribution of sizes of the prills (Table 1). Type A prills have about 25 mass % prills with a diameter of less than 1.7 mm. As discussed by Dallavalle [14], for a binary or multiple component system (of varied sizes of spherical particles), the smaller component can fit in the interstices of the larger component, hence increasing the bulk density. Systems of one size component are not amenable to as high a bulk density as are multiple component

systems, and binary systems do not reduce the void space as much as three or more component systems.

The higher bulk density enhances the wettability of Type A prills, in comparison with Types B and C prills (Table 1), while they have similar surface and structural properties. For Types D and E prills, the bulk density is higher than for Type A prills. However, their high bulk densities are due to their higher prill densities, that is, low porosities; the low porosity of Types D and E prills are the limiting factors for their wettability.

Effect of Particle Size. The surface area available for adsorption is dependent upon the particle size of the samples. The specific surface area for spherically shaped particles is inversely proportional to the particle diameters, and the surface area per unit volume increases very rapidly with a decrease in particle size, especially at smaller diameters. This results in a much larger surface area per unit volume of materials accessible for liquid adsorption.

To study the effect of particle size on wettability of AN prills, Type A prills were screened into four size ranges, and their wettability with heptane was determined using capillary penetration measurements. As compared in Table 3, there are no significant differences in the wetting rates of the samples. The wettability of AN prills seems to be weakly dependent on the prill size in this limited range.

The effect of particle size was further studied by using AN samples in powder form. The first powder sample (Powder 1)

Table 3
Wetting rate of type A prills of different sizes with heptane

Prill size/mm	10^3 Wetting rate/g^2 min^{-1}
1.0–1.4	2.22 ± 0.16
1.4–1.7	2.65 ± 0.22
1.7–2.0	2.65 ± 0.26
2.0–3.0	2.61 ± 0.15

was ground from Type A AN prills, and the second one (Powder 2) was obtained by breaking down temperature-cycled prills. For the powders the wetting rate of heptane is fast, and it is difficult to monitor the penetration rate precisely. Consequently the comparison of the wettability of prills and powders was conducted with the wetting rate of hexadecane; the results are listed in Table 4.

The wetting rate of Powder 1 (Table 4) is about a factor of 180 greater than that of Type A prills (Table 2). The wetting rate is further increased with Powder 2 ($\sim$ a factor of 500), which has a finer particle size. As shown in Table 4, the particle size for Powder 1 was largely between 250 and 600 μm, and that for Powder 2 is between 125 and 250 μm. In Table 4 the particle size distributions for both samples were determined by sorting the powders through sieves with various sizes.

With finer particles, the total surface area of the samples for adsorption is higher. Hence, the wettability of AN increases as the particle size decreases. Finer powders have substantially higher wettability than AN in prill form. However, they also have greater tendencies to absorb moisture and to cake, thereby limiting the adsorption of fuel oil. Moreover, X-ray microanalysis shows that the surfaces of the ground powders contain oxygen, nitrogen, and sulfur. Compared to Type A AN prills (Table 1), the ground powders have less impurity on their surface, since the prills' interior is exposed after grinding. The difference in surface composition may contribute to the increased

Table 4
Particle size distribution of AN powders and their wetting rate with hexadecane

Powder	Particle sizes/μm				10^3 Wetting rate/ $g^2\ min^{-1}$
	38–125	125–250	250–600	>600	
1	5.2	26.5	57.7	10.5	75 ± 8
2	9.0	44.4	26.7	19.9	214 ± 18

wetting rate. If AN prills could be ground immediately prior to the application, or if the prill is friable enough to break down during pneumatic loading, a substantially higher wetting rate may result.

Wettability of Treated Prills

Effect of Moisture. Studies were carried out on the effect of moisture content on the wettability of AN with alkanes. The moisture content of the as-received and moisturized prills was determined by measuring water desorption from the samples using TG. A plot of typical TG results for moisture analysis on moisturized prills is illustrated in Figure 7. The moisture contents of the samples were compared using the total mass loss at 100°C (Table 5). The error terms represent one standard deviation obtained from at least two replicates. The moisture content is a function of the time exposed to water vapor and the R.H. in the system. For the AN prills exposed to water vapor for more than 18 hours, the samples were dissolved, since AN is hygroscopic and readily soluble in water.

The wetting rate of the various moisturized AN samples with heptane was determined using the capillary penetration technique. As shown in Figure 8, the results from the capillary rise measurement show that the wettability of AN prills decreases linearly with increasing moisture content.

The lower wettability may be caused by blockage of the pores and the surface of AN prills by water, or even by dissolving the prill surface, as shown in Figure 9a with a prill exposed to moist air for 12 hr. Prills moisturized for a shorter period may not be seriously affected. However, the adsorbed water may still increase the hydrophilic property of AN prills and increase the contact angle of AN with alkanes, thereby preventing the alkanes from entering the pores of AN prills.

Effect of Temperature Cycling. To investigate the effect of temperature cycling on the wettability of AN prills, capillary penetration measurements of T-cycled and cold-treated (dry ice, −78°C) prills were attempted. However, as illustrated in

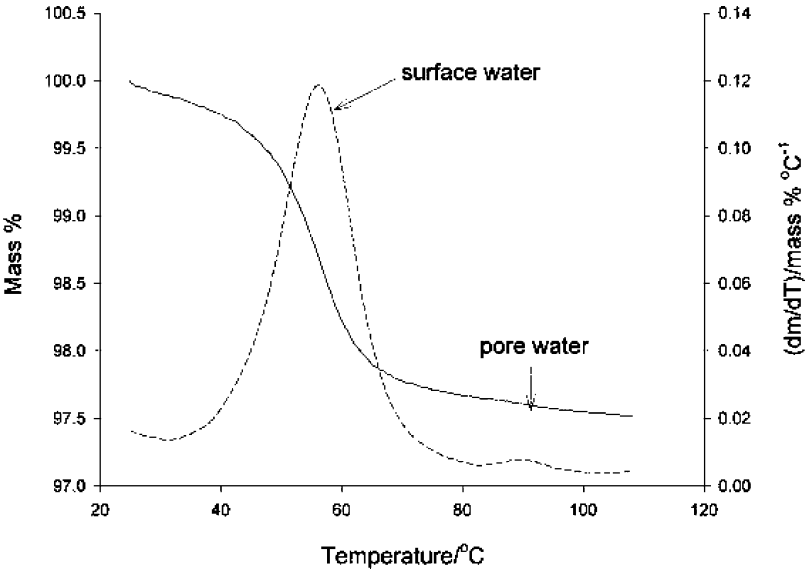

Figure 7. Typical TG results for moisture content analysis. *Solid line*: mass; *dashed line*: derivative of mass with temperature.

Figure 9b, the prills degrade very easily, ultimately leading to disintegration or powdering after the temperature cycling. Capillary penetration measurements could not be performed with samples remaining in the prill form, because the samples

Table 5
TG results for moisture analysis of AN prills

Time of moisturizing/hr	Moisture content/mass %
0	0
1.5	0.46 ± 0.03
3	2.18 ± 0.04
5	1.10 ± 0.10
6	2.42 ± 0.11
12	3.79 ± 0.13

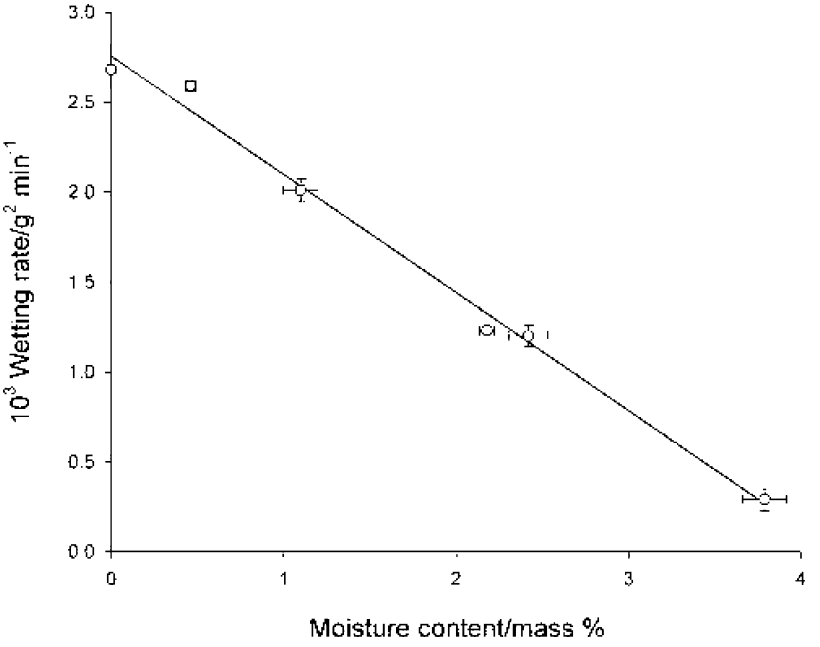

Figure 8. Effect of moisture content on wettability of AN prills. Error bars show standard deviation of at least two replicates.

could not withstand normal handling, even with very gentle loading into the tube.

The disintegration of AN prills is caused by a structural and volume change as a result of the low-temperature phase transition at −34°C, since no disintegration was observed from the cold-treated (freezer, −22°C) and the heat-treated prills. There are no published crystal lattice data for AN phase VI [15]. This low-temperature phase transition may result in unwanted prill fracture when winter conditions result in temperatures lower than −35°C.

The capillary penetration measurements were also conducted on the cold-treated (freezer, −22°C) and the heat-treated AN prills. No change in wetting rate was observed from the cold-treated sample, whereas the wetting rate of the heat-treated prills ($4.49 \pm 0.28 \times 10^{-3}$ g^2 min^{-1}) is 70% higher than

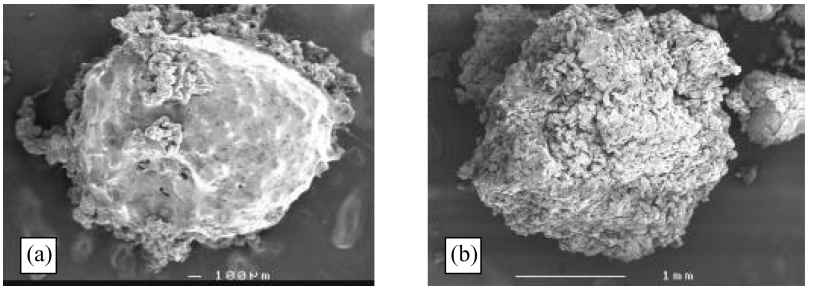

Figure 9. SEM micrograph of (a) moisturized AN prill, (b) temperature-cycled prill.

the as-received prills ($2.68 \pm 0.05 \times 10^{-3}$ g^2 min^{-1}). There are two possible reasons for the enhanced wettability: (1) a lower moisture content, and (2) a morphology change in heat-treated prills due to a IV–II or IV–III phase transition.

If the substantial difference in wettability between the as-received and the heat-treated prills is due primarily to the moisture content, their difference in moisture content would be 2.65 mass %. This value was estimated by extrapolating the linear relationship between the wettability and the moisture content in Figure 8. The TG results have shown that there is no water on the surface and in the pores of the as-received prills. Additionally there is no significant increase in the wetting rate of a desiccated sample prepared by placing it in the desiccater under vacuum for 14 days. Thus, it appears that the increased wettability results from a morphology change of the AN prills, probably the IV–II phase transition, which occurs in the heat-treated sample.

Conclusions

The capillary penetration technique involves application of the Washburn equation to determine experimentally the rate of penetration of a liquid into a particle bed. The main deficiency of the model on which the Washburn equation is based is that only a single cylindrical capillary is used to characterize a complex

porous network. Hence, the method cannot properly model the exact pathway of the liquid penetration in AN prills. However, the wetting rate data can be used as an empirical measure to compare the relative wettability of various AN prills. The sensitivity and simplicity of the capillary penetration technique make it useful for comparing the wettability of samples.

The wettability of various AN prills with alkanes and fuel oil was compared. Factors influencing the wettability of AN prills include surface tension, viscosity, density, and purity of the wetting liquid, as well as surface composition, porosity, bulk density, particle size, size distribution, moisture content, and thermal history of AN samples. The explosive-grade (porous) AN prills show a better wettability due to combined effects of the above factors.

The wetting rate of AN powder is about 500 times that of normal prills. Finer powders have substantial higher wettability than AN in prill form. However, they also have higher tendencies to absorb moisture and to cake, which prevent the adsorption of fuel oil. The reduction in size must be carried out immediately before wetting if the advantages of a higher wetting rate are to be consistently obtained.

The capillary penetration results show that the wettability of AN prills decreases linearly with increasing moisture content. For the effect of temperature, disintegration was observed from prills cycled through the V–VI phase transition. On the other hand, prills passed through the IV–II phase transition have wetting rates that are 2.5 times that of as-received prills. The enhanced wettability may be due to the morphology change in the prills.

Acknowledgments

The authors thank Ms. Aida Kaldas at Orica Canada Inc., Mr. Gordon Chalmers at ETI Canada Inc. and Dr. Merv Fingas at Environment Canada for sample donations; Dr. Robert Burk and Dr. Bio Aikawa for suggestions on sample analysis; and Mr. Lew Ling for conducting the SEM measurements.

References

[1] Maranda, A., D. Galezowski, and M. Swietlik. 1998. *Przegląd Gˊrniczy,* 54(11): 33.
[2] Rowland, J. H., III, and R. Mainiero. 2000. *Proceedings of the 26th Annual Conference on Explosives and Blasting Technique,* Anaheim, CA, 1: 163.
[3] Mader, C. L. 1998. *Numerical Modeling of Explosives and Propellants,* Boca Raton: CRC Press.
[4] Davey, R. J., P. D. Guy, B. Mitchell, A. J. Ruddick, and S. N. Black. 1989. *J. Chem. Soc., Faraday Trans. I,* 85(7): 1795.
[5] Rouquerol, F., J. Rouquerol, and K. Sing. 1999. *Adsorption by Powders and Porous Solids,* San Diego: Academic Press.
[6] Li, D. and A.W. Newmann. 1996. *Applied Surface Thermodynamics,* ed. A. W. Newmann and J. K. Spelt , New York: Marcel Dekker, 557.
[7] Prestidge, C. A. and G. Tsatouhas. 2000. *International Journal of Pharmaceutics,* 198: 201.
[8] Shi, S. Q. and D. J. Gardner. 2000. *J. Adhesion Sci. Technol.,* 14(2): 310.
[9] Washburn, E. W. 1921. *Phys. Rev.,* 17: 273.
[10] Siebold, A., A. Walliser, M. Nardin, M. Oppliger, and J. Schuetz. 1997. *J. Colloid Interface Sci.,* 186: 60.
[11] Quéré, D. 1997. *Europhys. Lett.,* 39: 533.
[12] Chattopadhyay, A. K., J. Knight, R. D. Kapadia, and S. K. Sarkar. 1994. *Journal of Materials Science Letters,* 13: 983.
[13] Kwok, Q. S. M. and D. E. G. Jones. 2001. *Proceedings of the 29th North American Thermal Analysis Society Annual Conference,* St. Louis, Missouri, 633.
[14] Dallavalle, J. M. 1948. *Micromeritices,* New York: Pitman Publishing Co.
[15] Shehap, A. M. 1999. *Egyptian Journal of Solids,* 22(1): 107.